Shrinkage behaviour of low-profile unsaturated polyester resins

Mark Kinkelaar, Bing Wang and L. James Lee*
Department of Chemical Engineering, The Ohio State University, Columbus, OH 43210, USA
(Received 19 November 1993)

A dilatometer, designed and built in-house, was applied to the study of low-profile unsaturated polyester resins. The change in polymer morphology as a function of polymerization shrinkage and low-profile additive (LPA)-induced plateau region, and the role of fissure formation in the LPA mechanism were investigated. An LPA mechanism was proposed based on the findings of this study. Also included in this work was the effect of pressure and thickening on shrinkage control. Finally, a series of bulk moulding compound compression mouldings was performed to investigate the relationship between polymerization shrinkage control and moulded panel surface quality and moulding shrinkage.

(Keywords: unsaturated polyester resin; low profile additive; shrinkage control)

INTRODUCTION

Low-shrink and low-profile unsaturated polyester (UP) resins are commonly used in several reactive processing manufacturing techniques, such as compression moulding of sheet moulding compound (SMC) and bulk moulding compound (BMC), resin transfer moulding (RTM), pultrusion, hand lay-up and resin casting processes. As these processes share a common resin, they also share some common manufacturing problems which have hindered growth in their respective markets[1–8]. These problems include surface quality flaws such as sink-mark formation and part-surface waviness, and dimensional control problems such as warpage and inability to accurately reproduce the mould (mould shrinkage or dimensional control). All these problems are due to, at least in part, the UP resin's polymerization and thermal shrinkages.

The key method used to reduce polymerization shrinkage of this system is the inclusion of a low-profile additive (LPA) in the resin formulation. The purpose of the LPA is to compensate for the thermal and polymerization shrinkage of the UP resin at a minimum cost to other cure properties, such as product strength and stiffness, reaction rate, etc. For non-cosmetic applications the LPA is most often omitted from the formulation. The LPA is a thermoplastic material which is compatible, or partially compatible, with the styrene and UP resin mixture before cure and becomes incompatible at some time during cure. The LPA (most often) does not participate in the free-radical polymerization; however, it is known to have an effect on compound viscosity and thickening[3,9–11].

Standard low-shrink additives and LPAs include polyethylene (PE)[3,12], polystyrene (PS)[3,12,13], poly(vinyl acetate) (PVAc), poly(methyl methacrylate) (PMMA)[3,9,13,14], polymers prepared from ε-caprolactones[2,15], poly(styrene-*co*-butadiene)[11,12], polyurethanes[3,13,14,16], copolymers with acrylates[3] and other less common thermoplastics. Among them, PVAc- and PMMA-based LPAs are most widely used. The amount of LPA used in the formulation depends on the application and is usually determined by trial and error. The optimum amount varies for different LPAs, unsaturated polyester resins and reaction conditions.

Some other factors to consider in selecting an LPA are its molecular weight, dipole moment and glass transition temperature, T_g. The molecular weight of the LPA has been shown to have a useful range which is LPA specific. For the case of PVAc[3], the useful range is 10 000–250 000, and preferably between 25 000 and 175 000. Good shrinkage control has been correlated with the dipole moment of the LPA[17]. The dipole moment of uncured polyester resin was estimated to be 2.0–2.5, while that of the cured resin was estimated to be 0.2–0.8. The dipole moment was determined to be 1.6 for PVAc and only 0.3 for PS. It was hypothesized that an LPA with a large dipole moment would be very compatible with the highly polar unreacted resin; however, on cure the LPA becomes increasingly incompatible with the resin due to the large difference in polarity. In essence, the difference in dipole moment would act as a driving force for phase separation[3,17]. For the case of PVAc, this seems to be true. For a less polar LPA, one should expect that the driving force for phase separation is less and that LPA performance should decline, as has been shown by PS performance as an LPA[3].

Although the detailed LPA mechanism for controlling polymerization shrinkage is still not well understood, a general explanation based on information available in the literature can be summarized as follows[2,3,17]:

1. As the material is heated it expands thermally.
2. The rise in temperature causes initiator decomposition and cure starts.
3. The once compatible thermoplastic becomes incompatible and starts to form a second phase.

* To whom correspondence should be addressed

0032-3861/94/14/3011–12

4. Unreacted styrene and UP resin start to collect in the thermoplastic phase.
5. Temperature and degree of polymerization continue to increase. As the degree of polymerization increases, the UP phase shrinks. As the temperature increases, the volume occupied by the LPA and unreacted monomer increases, compensating for polymerization shrinkage.
6. The monomer in the LPA phase starts to react, creating microvoids in that region due to the polymerization-induced stress. Alternatively, some researchers have proposed that the polymerization shrinkage in the UP phase causes a large stress to occur in the LPA phase, which leads to microvoids in the LPA phase[16].
7. Finally, part cooling occurs. Above the T_g of the UP resin phase, the bulk coefficient of thermal expansions of the LPA phase and the UP phase are about the same. Below the T_g of the UP phase, the UP phase will shrink much less on cooling than the LPA phase. This difference in cooling shrinkage will cause more microvoids to occur in the LPA phase as more stress is applied over the LPA phase, and this will continue until the T_g of the LPA phase has been reached.

Further complicating the LPA mechanistic studies is the common inclusion of thickeners in compounds used for compression moulding. Thickeners are additives used to increase compound viscosity which in turn provides for ease of handling and fibre carry during compression moulding[2,3,9,10,12,18–26]. In addition, the use of a thickener enables the compounder to use a less viscous system to compound, providing for higher glass fibre and filler loads.

The most common method of thickening is the use of the alkaline earth oxides and hydroxides, especially magnesium and calcium oxide and hydroxide. The exact reaction mechanism still remains unclear[2,3,12,20,23]; however, the literature agrees that the acid groups in the resin react with the alkaline earth. According to polymerization theory, the rise in viscosity is too large for such a limited increase in molecular weight, therefore it has been proposed that some sort of ionic orientation or aggregation plays an important role in thickening[12].

During the early development of LPAs, it was found that the low-profile resin became sticky or tacky on thickening, owing to the LPA becoming incompatible with the thickened resin[3]. To counteract the undesired separation, carboxyl groups were added to the LPA thermoplastic. This caused the LPA to participate in the thickening reaction and prevented separation before cure[3,27]. What is not clear, and of interest in this work, is the effect this has on the LPA mechanism.

To better understand the LPA mechanism, it is necessary to measure the polymerization shrinkage during cure. Traditionally, a dilatometer is used to measure the pressure–volume–temperature relationship of a material. For thermoset polymers, such as UP resins, conversion is also a variable so one needs to measure the pressure–volume–temperature–conversion (reaction) relationship. Although some dilatometry data have been obtained for low-shrink and low-profile UP resins[28,29], most of the work was preliminary in nature, comparing only samples with and without LPA[28] or varying LPA type[29], but not being too concerned about the LPA mechanism. In addition, most of the dilatometers in the literature are hindered by their inability to successfully handle reaction exotherm due to sample geometry. The purpose of this study is to determine LPA performance as well as to provide a better understanding of the LPA mechanism using a dilatometer designed and built in-house.

INSTRUMENTATION

This study relied on four instruments: a differential scanning calorimeter (d.s.c.); a scanning electronic microscope (SEM); a BET surface area measurement apparatus; and a dilatometer developed earlier in our laboratory. The d.s.c. used was a TA Instruments DSC 10. All samples were reacted in an aluminium volatile sample pan, which was capable of withstanding an internal pressure of 0.2 MPa (2 atm) when sealed. D.s.c. sample size was approximately 10 mg and an empty pan was used as a reference. The SEM used was a Hitachi S-510 with 25 keV power. SEM samples were prepared by fracturing, etching in dichloromethane and gold coating for 60 s, unless noted otherwise. The BET apparatus used was a Micromeritics 2100E Accusorb system. Krypton was used as the adsorbate and the samples were outgassed overnight at approximately 100°C before surface area measurements were performed. Finally, a brief description of the dilatometer is offered here; a more thorough description has been given elsewhere[30].

A cut-away view of the dilatometer configuration is shown in *Figure 1*. The lower half of the dilatometer, including the cavity between the two discs and the lower half of the hydraulic cylinder, was the sample chamber. With the lower valve closed, the sample chamber was a

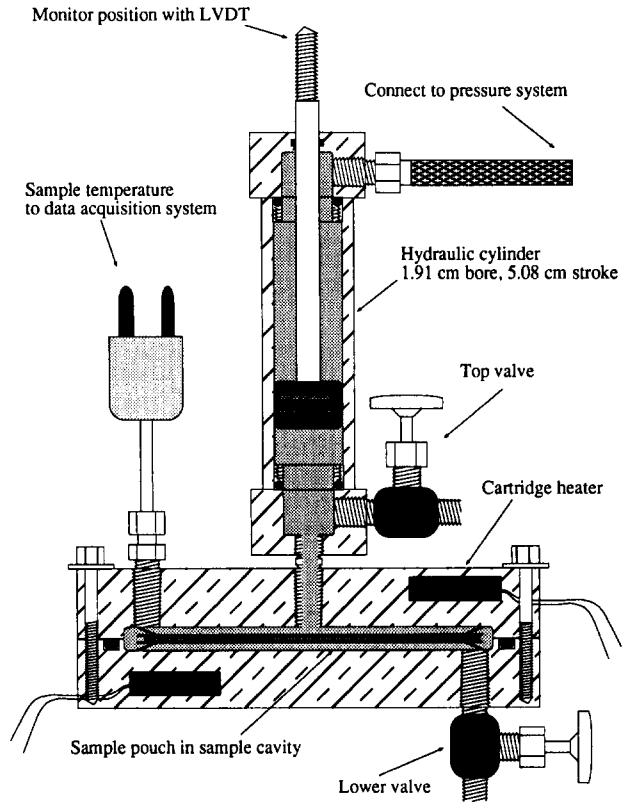

Figure 1 Schematic of dilatometer[30]

closed system. The sample chamber contained both the sample (sealed in a plastic film pouch) and the encapsulating fluid (Dow Corning 550 fluid). The upper part of the hydraulic cylinder was also filled with the Dow Corning 550 fluid and it was attached to a constant pressure source, thus pressurizing the sample chamber. Any volumetric changes in the sample or encapsulating oil (sample chamber), including thermal effects and polymerization shrinkage, were measured by following the change in position of the hydraulic cylinder rod. To obtain the polymerization shrinkage as percentage volume change, first the cure heating cycle was performed, then the heating cycle was repeated to get the thermal response for both the sample and the encapsulating oil (baseline). The percentage volume change was calculated by subtracting the baseline from the cure response and accounting for the sample volume and hydraulic cylinder geometry[30].

DILATOMETRY EXPERIMENTS

The major objective of this work is to study the effect of pressure and thickening on LPA performance as well as to determine the LPA mechanism and how it is related to moulded part-surface quality and moulding shrinkage. In a previous paper[30], the effects of cure temperature history and LPA concentration were investigated, and the results of that study will be discussed later in this work with regard to the moulding series presented. First, the effects of pressure and thickening on LPA performance are presented, followed by the determination of the LPA mechanism. Finally, the moulding results are discussed in light of the proposed LPA mechanism.

Materials and formulation

Typical UP resin compounds often include the unsaturated polyester resin, styrene, LPA, initiator, inhibitor, filler, thickener, fibre, mould release agent, etc. To minimize the amount of variables and to avoid confusing and unnecessarily complicated results, only a UP resin, styrene, an LPA and one initiator were included in the formulation.

The UP resin used was Ashland Chemical's Q6585. It was manufactured from a 1 to 1 molar ratio of maleic anhydride and propylene glycol. There were an average of 10.13 carbon–carbon double bonds per UP molecule. The UP had an average molecular weight of 1580 g mol^{-1}, which worked out to be about 156 g mol^{-1} of UP C=C. The resin was shipped as a 65% solution of UP in styrene. The LPA used was Union Carbide's LP40A, which was a 40% solution of acrylic-modified PVAc in styrene. The compound was formulated to provide a styrene C=C to unsaturated polyester C=C ratio of 2.0. The LPA concentrations discussed later in this paper are weight percentage of solids based on the total weight of the UP resin, styrene and LPA. Unless otherwise stated, 1% PDO was used in the formulation as the initiator and no inhibitor was added. *Table 1* summarizes the compositions used.

Effect of pressure on shrinkage control

The effect of pressure was investigated by comparison of the high-pressure and low-pressure cure shrinkage profiles of two of the formulations in *Table 1*: the 2.5% and the 6% LPA formulations. Both samples were cured isothermally at 80°C in the dilatometer at 0.69 MPa (100 psi) and 2.55 MPa (370 psi) sample pressure. *Figure 2* is a plot comparing the per cent volume change *versus* time for the 6% LPA sample cured at high and low pressures. When comparing the data in *Figure 2* one must understand that a hysteresis problem occurred at high pressure with the current dilatometer design. The effect of this hysteresis is that the high-pressure data obtained were somewhat compressed. That is, the high-pressure data shown in *Figure 2* should have shown a larger expansion before cure (during heating) and more shrinkage at the end of the heating cycle, aligning the high-temperature and low-temperature final shrinkage data. Nonetheless, the trends in the data and the final shrinkage measured are correct, as the baseline returned to the zero position for these experiments. The baseline was used to indicate the validity of an experiment; if it returned to the zero position no leakage

Table 1 Summary of the formulations used in this study

Formulation	Q6585 (g)	LP40A (g)	Styrene (g)	PDO[a] (g)
No LPA	65.9	0.0	34.1	1.0
2.5% LPA	64.25	6.25	29.5	1.0
5% LPA	62.6	12.5	24.9	1.0
6% LPA	61.9	15.0	23.1	1.0
10% LPA	59.3	25.0	15.7	1.0
15% LPA	56.0	37.5	6.5	1.0

[a] PDO, t-butyl peroxy-2-ethylhexanoate

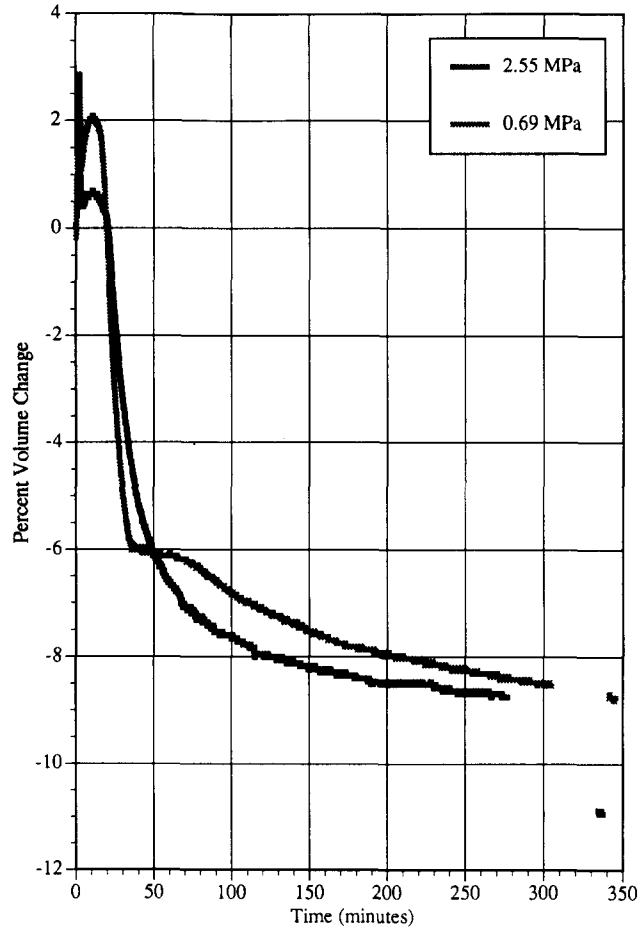

Figure 2 Effect of pressure on 6% LPA sample cured isothermally at 80°C

Table 2 Comparison of final shrinkage and colour/opacity for the pressure series

Sample	Appearance	Final shrinkage (%)
2.5%, 0.69 MPa	Two regions, stark white and translucent	7.8
2.5%, 2.55 MPa	Translucent	12.5
6%, 0.69 MPa	Stark white	8.8
6%, 2.55 MPa	Blotchy translucent	11.0

occurred and the results were valid, if not either more cure or a leak occurred.

Comparing the high- and low-pressure experimental results, the final shrinkage is markedly higher for the high-pressure sample. Furthermore, the plateau region was not observed at high pressure, as shown in *Figure 2*. The sample appearance was also different for the two samples. The low-pressure sample was stark white (opaque) in appearance and the high-pressure sample was blotchy and translucent in appearance. Similar observations were made for the 2.5% LPA sample (that is, the loss of the plateau region with pressure and the opaque sample at low pressure/translucent sample at high pressure) with the exception that the high-pressure sample did not turn opaque on etching. *Table 2* summarizes the pressure effect results for both samples. From these results, clearly, pressure had a negative effect on shrinkage control.

Figure 3 is a comparison of the sample morphology for the pressure studies. *Figures 3a* and *b* are the 6% LPA samples cured at 0.69 MPa (100 psi) and 2.55 MPa (370 psi), respectively. From these micrographs, pressure did not have a large effect on morphological development. The only difference visible was that the particles formed at higher pressure were slightly smaller.

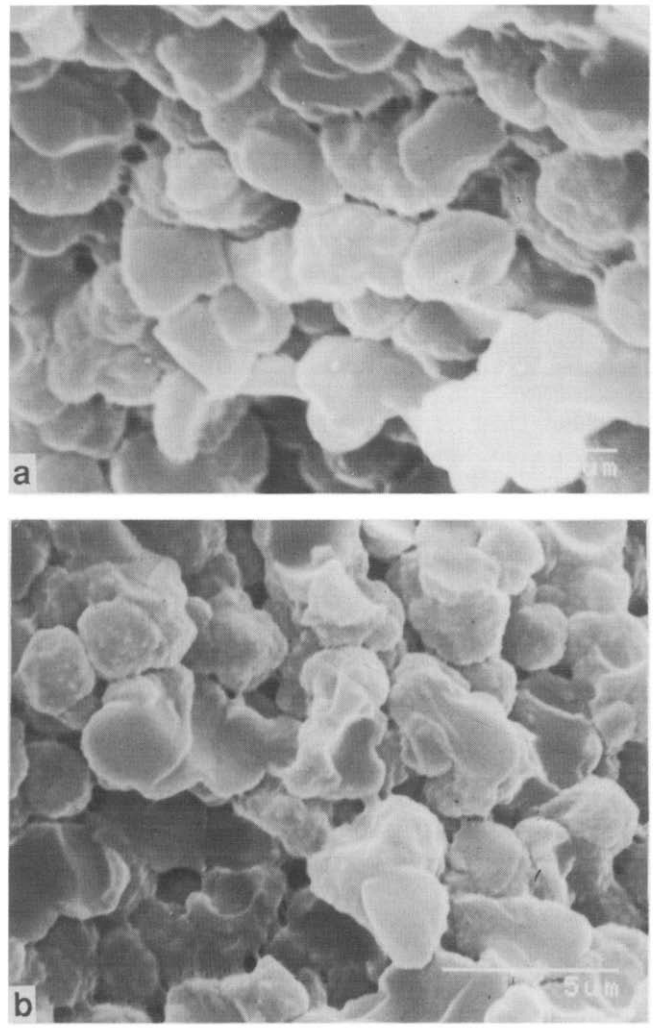

Figure 3 Morphology of the 6% LPA sample cured isothermally at 80°C: (a) 0.69 MPa; (b) 2.55 MPa

Effect of thickener

The effect of thickening on shrinkage control was investigated both isothermally and with a ramp heating profile. Ramp mode was performed using a Variac to provide a reduced voltage to the cartridge heaters used in the dilatometer. Ramp heating rate was adjusted by the Variac position and had a useful rate range of approximately 4–20°C min^{-1} with an operating temperature range of room temperature to 200°C. As discussed earlier, thickening is the ionic reaction between alkaline earth oxides and the carboxyl groups in the resin and sometimes in the LPA. In the case of the formulations used in this study, both the LPA and the UP resins used had carboxyl groups and therefore participated in the thickening reaction. The 6%, 10% and 15% LPA formulations in *Table 1* were used with the addition of 3% MgO by weight, and no filler was used to study shrinkage control of thickened samples.

Careful sample preparation was required to get repeatable results and a well-mixed sample. Sample preparation consisted of first formulating the resin and mixing well for approximately 20 min. Then the MgO was added, mixing it first with a small amount of the resin and then blending that into the rest of the batch. The sample was then mixed, first at a high shear to provide good mixing, then slowly to prevent separation, until the sample viscosity started to rise. The amount of time the resin took to start to thicken was highly dependent on LPA concentration: the 15% LPA sample started to thicken in about 2 h and the 6% LPA sample required over 6 h. Furthermore, formulations with more LPA provided the most uniformly thickened sample. The 6% and 10% samples would separate in the pouch if permitted to set, therefore they were strapped onto a high-speed shaker mixer (Thermolyte Type 50000 Maxi Mix III) to help prevent separation in these samples during the completion of thickening in the pouch. However, the 15% LPA sample, even without the mixer, still thickened more uniformly and therefore reacted slightly differently from the 6% and 10% LPA samples.

Figure 4 is a plot of per cent volume change *versus* time for the thickened samples isothermally cured at 80°C, 0.69 MPa (100 psi). Again, the difference in the 15% LPA sample and the 10% and 6% LPA samples may be attributed to sample uniformity. Comparing the 6% thickened sample to the 6% unthickened sample shown in *Figure 2*, it is clear that shrinkage control was lost by the inclusion of thickener. Furthermore, the samples were translucent in appearance, indicative of poor shrinkage control.

Figure 5 is an example of the ramp-cured thickened samples. It is a plot of per cent volume change *versus* time for the 15% LPA thickened samples cured at approximately 16°C min^{-1}. The secondary peak

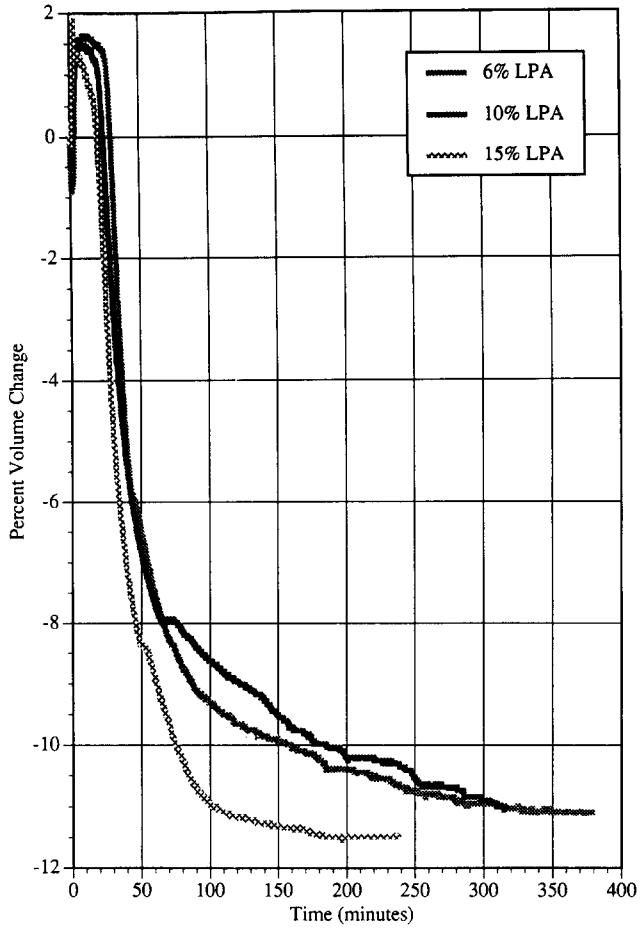

Figure 4 Comparison of per cent volume change *versus* time data of thickened samples with various LPA concentrations cured isothermally at 80°C

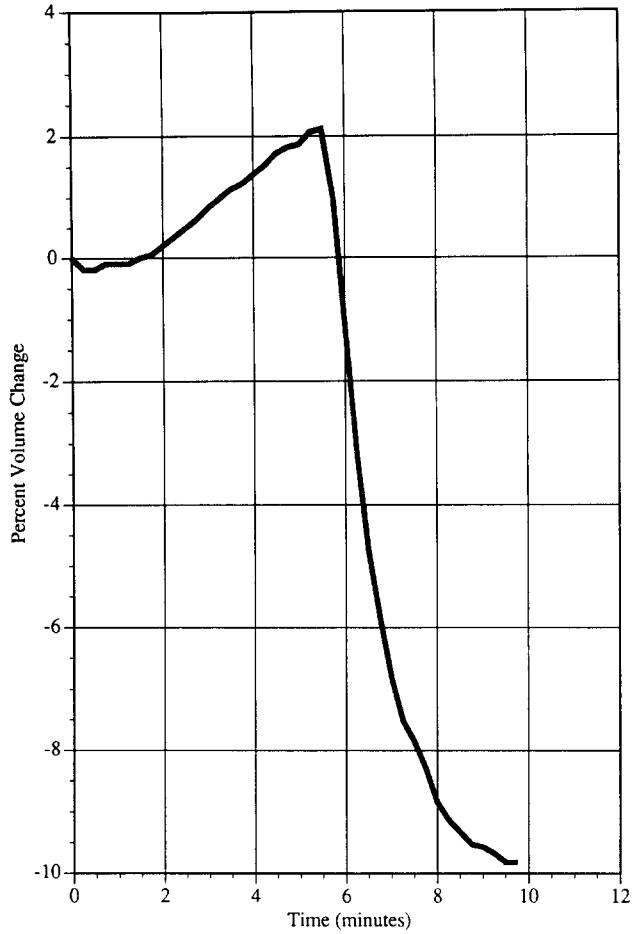

Figure 5 Per cent volume change *versus* time data of a thickened 15% LPA sample cured at 16°C min^{-1}

presented in the previous work[30] was not observed for any of these samples, and the corresponding temperature peak was somewhat smaller compared to the unthickened samples, approximately 10°C less. Some shrinkage control was observed for the ramp-cured samples; correspondingly, the samples were observed to be opaque in appearance.

Table 3 is a summary of the final shrinkages measured for the thickened samples. Some of the scatter in the shrinkage data should be attributed to sample non-uniformity. Clearly, shrinkage control was reduced with the inclusion of the thickener.

An explanation for the reduced shrinkage control can be found in the sample morphology, shown in *Figure 6*. *Figures 6a*, *b* and *c* are the 6%, 10% and 15% LPA isothermally cured thickened samples, respectively. The particulate morphology shown in *Figure 3* was not developed for these samples, though some microstructure was visible. The thickening reaction ionically coupled the UP resin and LPA molecules, changing the compatibility and the ability to phase separate during cure. This, in turn, prevented the particulate morphology formation and therefore the shrinkage control.

Comparing the morphology of the 6%, 10% and 15% LPA thickened sample cured at 8°C min^{-1} in *Figures 6d*, *e* and *f*, respectively, a particulate morphology was observed. The thickened sample morphology observed showed a much smaller particle size and a tighter packing structure when compared to the non-thickened counter part, which would explain the reduced shrinkage control.

Table 3 Summary of the final shrinkage data of the thickened samples. (Numbers in parentheses are the final shrinkage data of unthickened samples from ref. 30)

LPA content (%)	Isothermal final shrinkage	8°C min^{-1} final shrinkage	16°C min^{-1} final shrinkage
6	11.6 (9.9)	8.9 (3.5)	–
10	11.4 (10.1)	9.8 (4.7)	–
15	12.1 (9.8)	8.4 (5.0)	9.3 (4.8)

In the literature[31], it has been reported that the viscosity of thickened samples decreased greatly at approximately 100°C, implying that at least some of the ionic bonds that caused the thickening split at around 100°C. The reaction temperature peak was observed to start at around 110°C, therefore shortly before the reaction some of the ionic thickening bonds split, permitting some phase separation to occur and thus a particulate morphology to develop, to some extent. Comparing the 15% LPA 16°C min^{-1} thickened sample in *Figure 6g*, the particulate morphology was not so well developed as the 8°C min^{-1} sample and shrinkage control decreased accordingly, as shown in *Table 3*. At a higher heating rate, the time between splitting the ionic bond and gelation was reduced, therefore particle formation may have been limited by lack of time.

Summarizing, thickening had a negative effect on shrinkage control. It made particle formation difficult above the temperature at which the ionic bonds split and

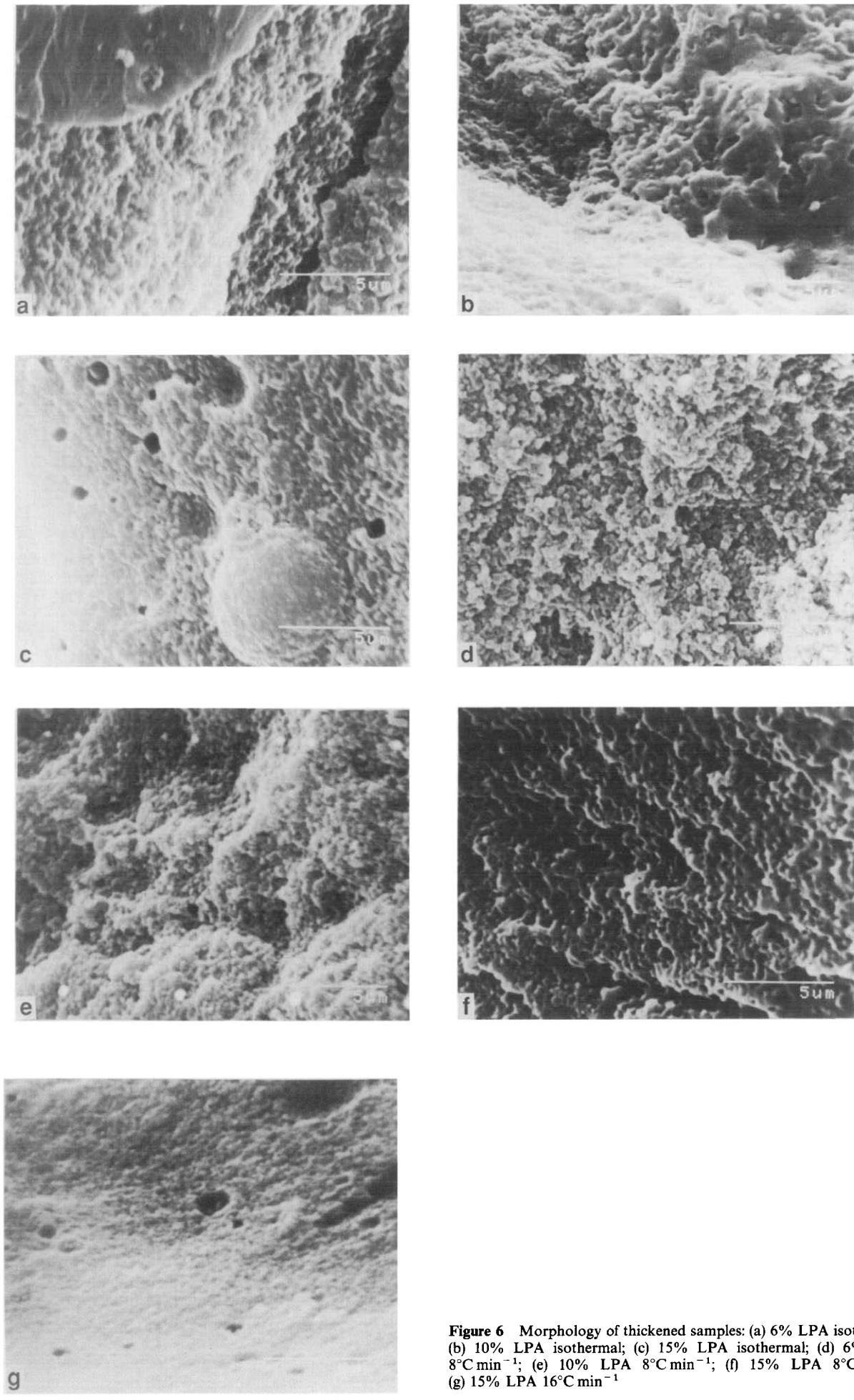

Figure 6 Morphology of thickened samples: (a) 6% LPA isothermal; (b) 10% LPA isothermal; (c) 15% LPA isothermal; (d) 6% LPA 8°C min^{-1}; (e) 10% LPA 8°C min^{-1}; (f) 15% LPA 8°C min^{-1}; (g) 15% LPA 16°C min^{-1}

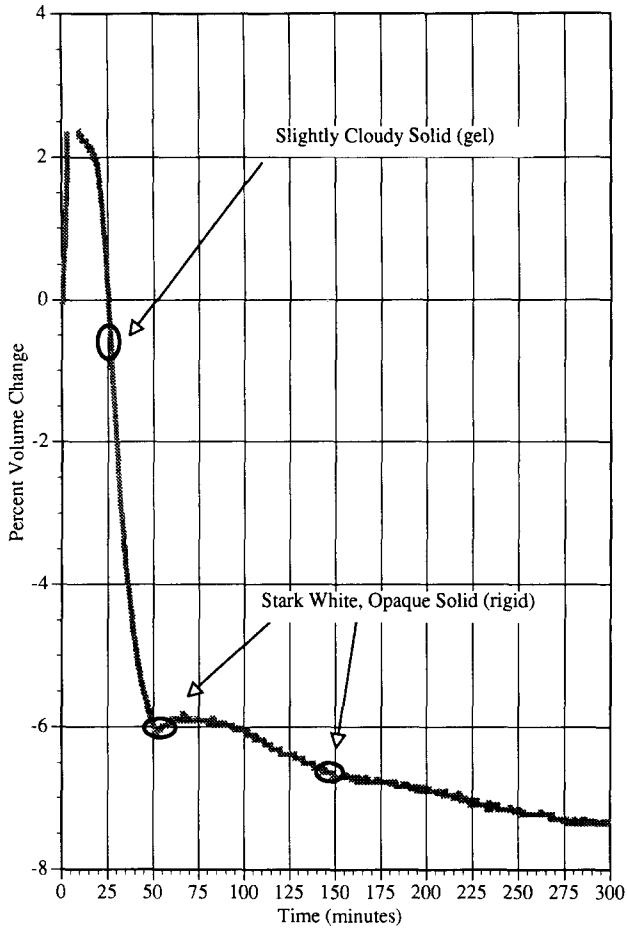

Figure 7 Per cent volume change as a function of time for 2.5% LPA sample cured isothermally at 80°C, 0.69 MPa

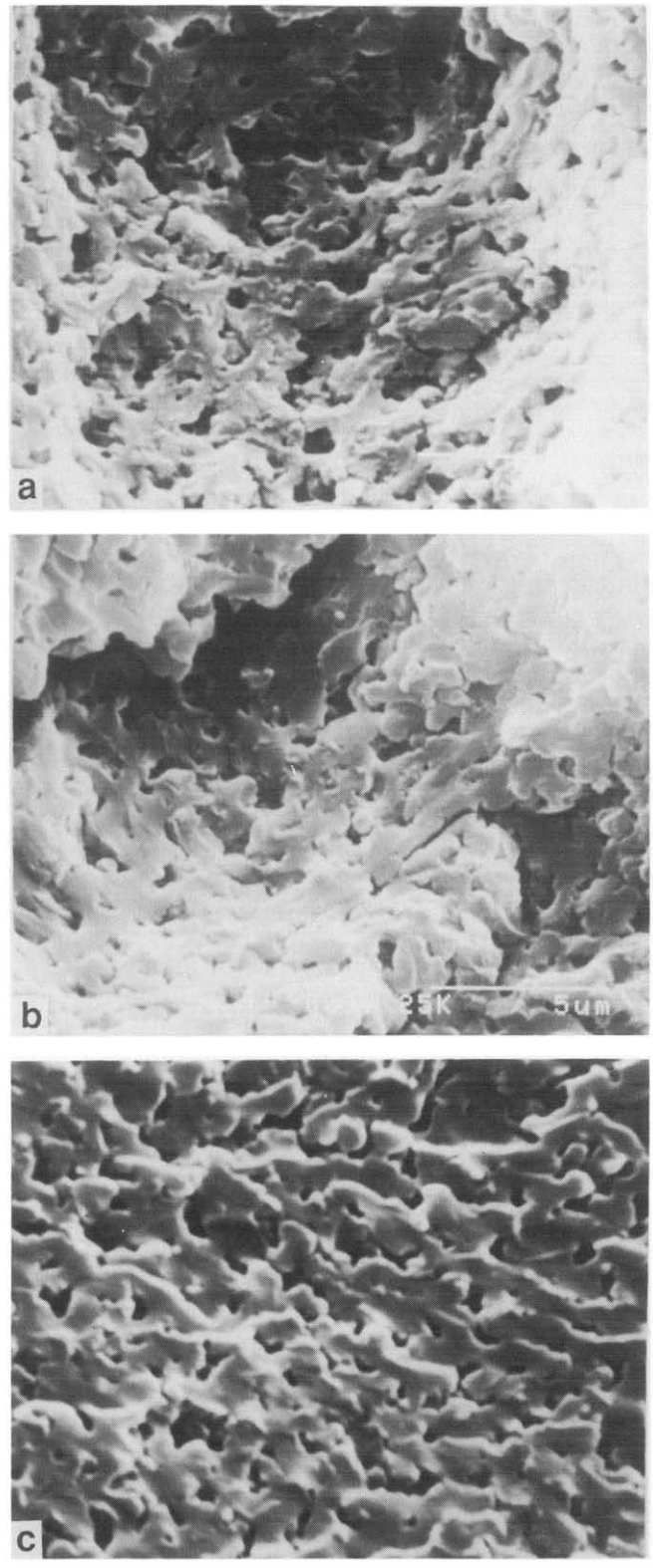

Figure 8 Change in morphology during cure of 2.5% LPA sample: (a) 26 min; (b) 50 min; (c) 150 min

impossible below that point. This, in turn, reduced the shrinkage control.

Change in morphology/opacity during cure

After developing an understanding of the effect of LPA concentration, heating rate and sample morphology on shrinkage control, it was deemed instructive to find how morphology changed during cure, especially before, during and after the plateau region shown in the isothermal data[30]. To accomplish this, the dilatometer experiment had to be stopped, the hot dilatometer disassembled and the sample removed and etched, first in a solution of dichloromethane with 3% *p*-benzoquinone (an inhibitor) and then in clean dichloromethane. The entire process took approximately 5 min from cutting the power to the heater, to placing the sample into the dichloromethane solution. The 2.5% LPA sample cured isothermally at 80°C, 0.69 MPa (100 psi), was chosen for this study, as it had the longest plateau region[30]. The reaction was stopped three times during the cure, at 26, 50 and 150 min into the experiment, as shown in *Figure 7*, and the sample appearance (opacity) and morphology were observed. The morphologies of the samples at the three points of interest are shown in *Figure 8*.

The first sample (26 min), corresponded to the region of large shrinkage before the plateau region. The 26 min sample was observed to be a slightly cloudy gel (solid). After etching, the sample turned stark white (opaque). The morphology of this sample is shown in *Figure 8a* and appeared slightly deflated, but nonetheless fully developed. This could be due to the removal of unreacted UP and styrene from the sample during etching, analogous to letting some of the air out of a balloon.

The 50 min sample, which corresponded to the beginning of the plateau region, was observed to be an opaque (stark white) solid. The corresponding morphology is shown in *Figure 8b* and is not markedly

different from the 26 min sample. Finally, the 150 min sample, representing a point after the plateau region, was also found to be an opaque solid and the corresponding morphology, which was not unlike the 26 and 50 min sample morphologies, is shown in *Figure 8c*.

Summarizing, the sample morphology did not change markedly after gelation, which occurred early on in the reaction; this is in agreement with some of the findings in the literature[32,33]. Opacity did change during the reaction, and shrinkage control, as demonstrated by the plateau region, corresponded to an opaque sample.

LPA mechanism

From the data presented in this work and ref. 30, it is clear that the sample morphology was important to the LPA mechanism, but in itself morphology did not fully explain the shrinkage control mechanism. This implies a two-step mechanism, requiring that microstructure formation occurs first. It has been proposed that fissures or voids form in the weaker LPA phase; however, little conclusive evidence for fissure formation was available. Fissure formation could explain why the samples with good shrinkage control (as measured by the dilatometer) are opaque or stark white in appearance, whereas the samples with poor shrinkage control (LPA acting as a non-reactive filler) were cloudy or translucent in appearance.

To investigate the occurrence of fissures in systems exhibiting shrinkage control, BET surface area analysis was performed on samples with various levels of shrinkage control. As LPA shrinkage control increased, fissure formation should have increased, if fissure formation is the second step in the LPA mechanism, and therefore surface area should have increased. Shrinkage control and surface area should correlate with each other.

BET[34–36], named after Brunauer, Emmett and Teller, is a technique used to measure the surface area of, most often, a catalyst, but any clean, non-volatile material may be used. The technique requires that the samples be outgassed entirely (overnight), preferably while being heated. Once all the gas adsorbed on the surface of the sample was removed, the samples (in glass vials) were placed in liquid nitrogen and a known amount of adsorbate gas was released into the sample chamber. Several gases were available as the adsorbate, including argon, nitrogen and krypton. Krypton was used for this study, as it was most applicable to the surface area range of interest (less than $2\ m^2\ g^{-1}$). The technique assumes that the first layer molecules to adsorb onto the sample surface were attracted by van der Waal forces, whereas additional layers were added by condensation. The amount of adsorbate gas was incrementally increased, measuring the equilibrium pressure for each known amount of gas. At equilibrium, the rate at which gas condensed and evaporated from the surface was equal. By equating the rates and summing over an infinite number of layers[34,35]:

$$V_a = \frac{V_m C P}{(P_s - P)[1 - (C-1)(P/P_s)]}$$

where V_a = volume of gas adsorbed at pressure P, V_m = volume of gas adsorbed when surface is covered with a monolayer, C = constant based on adsorbing gas type and temperature, and P_s = saturation pressure.

Rearranging:

$$\frac{P}{V_a(P_s - P)} = \frac{1}{V_m C} + \frac{C-1}{V_m C}\frac{P}{P_s}$$

So a plot of $P/V_a(P_s - P)$ *versus* P/P_s provided V_m, and from V_m the surface area of the material was found[34,35], knowing the area covered by one krypton molecule (21 Å^2).

Ideally, one might want to use 2.5% LPA samples isothermally cured along various regions of the shrinkage profile (before, during and after the plateau region), as was done for determining change in morphology during cure. However, this would not be possible owing to the presence of unreacted styrene in the sample. Therefore, the BET technique was applied to the 2.5% LPA isothermally cured high-pressure sample, the 2.5% LPA isothermally cured low-pressure sample and the 6% LPA sample cured at 8°C min^{-1}. The 2.5% high-pressure sample was chosen because no shrinkage control was observed, and the other two samples were chosen to represent various levels of shrinkage control.

The results of the BET studies are summarized in *Table 4*. It is clear that shrinkage control and surface area correlated nicely. Comparing the data in *Table 4*, a shrinkage control of 9.8% provided a 38-fold increase in surface area (between the high-pressure 2.5% LPA sample and the 6% ramp-cured sample) and a shrinkage control of approximately 3.5% provided a 2.5-fold increase in surface area (comparing the 2.5% low- and high-pressure samples). Note that the relationship between the surface area and shrinkage control is not linear. Studying the morphology of the low-pressure 2.5% LPA sample, it was evident that fissure development could not be well developed, therefore quite a few 'blind pores' should be expected. That is, all the fissures were not connected internally and pores existed in the centre of the sample, which were not accessible to the BET technique used.

Figure 9 shows SEM microphotographs of samples that were not etched and in which fissures were visible. *Figure 9b* shows the morphology of the ramp-cured 6% LPA sample used in the BET series of experiments, and *Figure 9a* shows the morphology of a 6% LPA sample cured isothermally at 80°C and 0.69 MPa (100 psi). Comparing the two, the fissures seemed to have developed in the LPA phase between the unsaturated polyester particles, as expected. However, the size and number of the fissures seem to be different. The isothermally cured sample showed a much larger, long and wide fissure through the particles, while the ramp-cured sample showed many much smaller, shorter and narrower fissures.

Given that the LPA mechanism is a two-stage process, including particle formation and subsequently fissure formation, the mechanism or cause behind fissure

Table 4 Summary of BET surface measurement experiments

	Sample		
	2.5% LPA, 2.55 MPa, iso. cure (80°C)	2.5% LPA, 0.69 MPa, iso. cure (80°C)	6% LPA, 0.69 MPa, scan (8° min^{-1})
Final shrinkage (%)	12.5	9.0	2.7
Surface area ($m^2\ g^{-1}$)	0.028	0.070	1.074

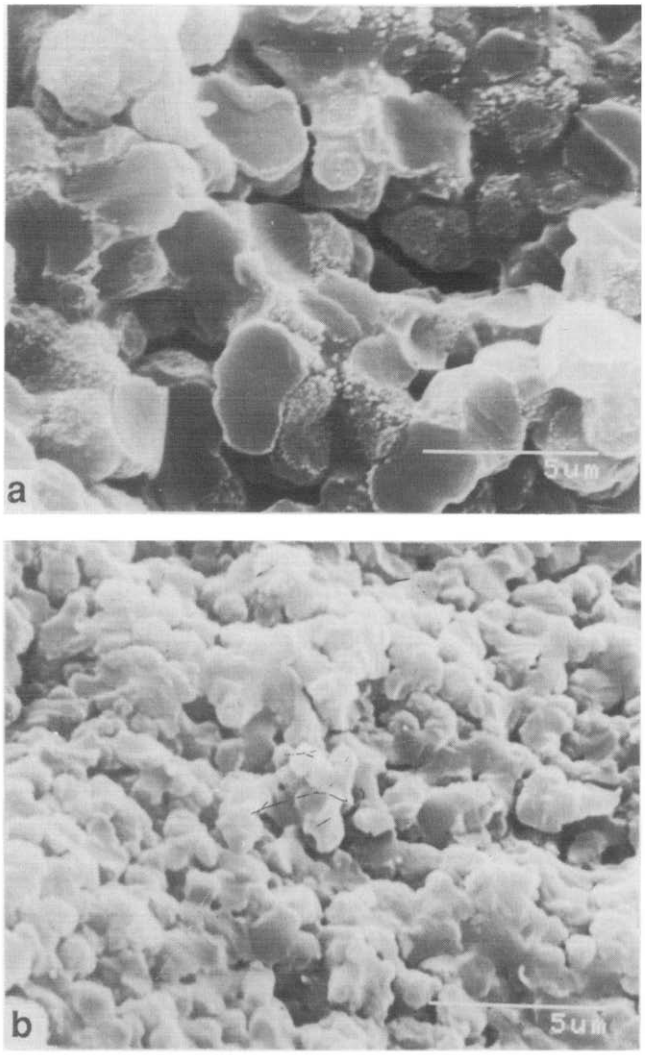

Figure 9 SEM microphotographs demonstrating fissure formation: (a) 6% LPA sample cured isothermally at 80°C and (b) 6% LPA sample cured at 8°C min^{-1}

formation still requires some explanation. Clearly, fissure formation did not occur in all of the samples, as some samples were translucent and shrinkage control was not observed. Fissure formation must have occurred because of internal stresses developed by the polymerization shrinkage and the level of stress necessary to develop the fissures must be different for different samples.

Reviewing the data in the previous sections of this work and ref. 30, the two-step mechanism can be applied to explain the shrinkage control observations. The relationship between LPA concentration and reaction temperature profile showed an optimal morphology, which was more loosely packed with larger and irregularly shaped particles. The larger, irregularly shaped particles and the looser packing structure provided the largest continuous weak phase in which the fissures could initiate and propagate. The faster reaction in the ramp-cure cycle provided a higher level of polymerization-induced internal stress owing to the fast reaction; therefore even though the weak phase was on a smaller order of magnitude, the internal stress developed could still cause the development of fissure formation. A slow reaction, as demonstrated by the isothermally cured samples, could permit stress-relaxation to occur, making fissure formation more difficult, even though the larger morphology would make fissure propagation easier[30].

The effect of pressure on shrinkage control can also be explained by fissure formation. It would be more difficult to form a fissure with the sample under pressure. Therefore, even though the sample morphology was not changed markedly by high pressure, fissure formation was more difficult. This may help to explain, at least in part, the benefits of using a two-stage moulding process in compression moulding. Initially, a high pressure in the mould is required for mould filling and good, intimate contact between the moulding compound and the mould. However, once the material has gelled and before the major reaction exotherm, it would be beneficial to release the mould pressure to help develop the fissures and control shrinkage.

Finally, the thickened sample data showed an underdeveloped morphology due to the ionic bonds formed during thickening. Despite the internal stress developed during the cure, the LPA phase did not develop as well as the unthickened samples and shrinkage control was affected accordingly. Both the development of the morphology and the development of internal-stress-induced fissures were required.

On the basis of the findings of this study, a proposed LPA mechanism is as follows.

1. As the material is heated it expands thermally, as indicated by the initial expansion observed.
2. The rise in temperature causes initiator decomposition and cure starts.
3. The once compatible thermoplastic becomes incompatible and starts to form a second phase. The UP resin develops the characteristic particulate morphology and the LPA forms a layer around and in between the UP particles. Morphology does not change markedly once developed. If the sample was thickened, most of the ionic bonds must first be split before morphology can develop.
4. The material becomes increasingly rigid as polymerization continues and internal stresses develop. At some critical internal stress value, fissures form along the weak LPA region and propagate.

MOULDING EXPERIMENTS

To investigate the role of shrinkage control in moulded part-surface quality and dimensional control, a series of BMC compression moulding experiments was performed using a formulation very similar to that used in dilatometry. All mouldings were performed by the Specialty Chemical Division of Union Carbide Corporation at South Charleston, WV, USA. One series of unthickened BMC compression mouldings was performed at 3.45 MPa (500 psi) moulding pressure using a 45.7 cm (18 in) square mould. The panels were moulded on a Lawtomatic 200 ton press (C. A. Lawton Co., De Pere, WI, USA) using a 1200 g charge. All samples were moulded for 4 min at 120°C.

The formulations in *Table 1* had to be changed slightly for moulding, including doubling the initiator concentration, the inclusion of filler, glass fibre and zinc stearate as an internal mould release agent. Glass content was kept low (10 wt%) in order to exaggerate the moulding shrinkage[3]. The filler used was Huber W4,

Table 5 Moulding formulations (based on weight)

Material	No LPA	2.5% LPA	6% LPA	10% LPA	15% LPA	20% LPA	25% LPA
Q6585	65.90	64.25	61.90	59.30	56.00	52.70	49.40
LP-40A (40%)	–	6.25	15.00	25.00	37.50	–	–
LP-40A (50%)	–	–	–	–	–	40.00	50.00
PDO	2.00	2.00	2.00	2.00	2.00	2.00	2.00
Zinc stearate	4.00	4.00	4.00	4.00	4.00	4.00	4.00
Styrene	34.10	29.50	23.10	15.7	6.50	7.3	0.59
Huber W4	200.0	200.0	200.0	200.0	200.0	200.0	200.0
PG-9033				10% glass by weight			

which was a 4 μm calcium carbonate powder. The glass used was Vetrotex P-276, which was a 1.25 cm (0.5 in) chopped fibre. Samples with 20% and 25% LPA were also prepared. In addition, one 15% LPA thickened formulation was prepared. The thickened sample was prepared by the inclusion of 2.0 phr of a MgO suspension (Plasticolors PG-9033) which worked out to be about 0.8 phr MgO overall. *Table 5* summarizes the formulations used for moulding.

The charges were prepared by first mixing the UP resin, styrene, LPA, mould release agent and initiator with a cowel mixer at high speed for 3 min. The filler was then added slowly and mixed for another 5 min. For the thickened sample, the thickener was added next and mixed for an additional 3 min. The resin was then transferred to a dough mixer (Hobart) and the glass was added and mixed for 2 min. Finally, the mixture was divided into the appropriate charge sizes, wrapped in a plastic film and then in foil and stored at room temperature overnight before moulding (except the thickened sample, which was stored overnight in a controlled environment at 27°C (80°F)).

D-sight results

A D-sight Audit Station-2 (Diffracto Co.) was used to quantify the moulded part-surface quality. The D-sight technique provided both a photograph of the part that emphasized the surface peaks and valleys and an unbiased index number related to the surface quality, which was larger for poorer quality surfaces and zero for an ideal, perfectly smooth, level, glossy surface[3]. The panels were used as moulded and no highlighting of the samples (application of a fluid to make the surface glossy) was necessary. The central regions of the parts were analysed consistently by placing each part on the same location of the sample table.

The no LPA and 2.5% LPA panels were by far the worst. The surface waviness was evident by visual inspection, and when placed on a flat surface warpage was very apparent. From the output, the D-sight index was very high for flat panels: 569.0 for the no LPA sample and 478.7 for the 2.5% LPA sample. The D-sight index numbers for this series are summarized in *Figure 10*. Finally, these two panels were different in colour compared to the other panels moulded. They were almost tan and fibres could easily be seen in the panel moulded without LPA. All the other panels were white in colour and fibre readout was not observed.

Continuing through *Figure 10*, the 6% and 10% LPA data showed continued improvement with addition of more LPA, the 15% LPA sample was slightly worse (with a slightly higher index) and again the 20% LPA sample

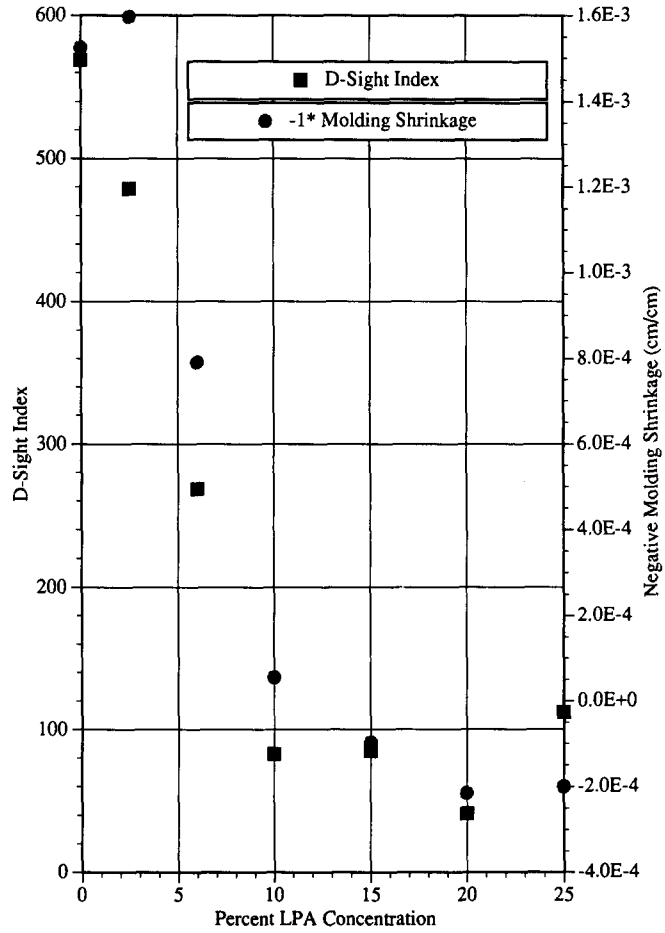

Figure 10 Comparison of D-sight index and moulding shrinkage as a function of LPA concentration

showed more improvement still. Finally, at the 25% LPA panel surface quality decreased markedly with increasing concentration. With moulding, several variables are important to surface quality, including the ability for the moulding compound to distribute evenly and carry fibres. As the LPA content increased, the viscosity of the resin increased and the shrinkage control increased, to a point. When viscosity is too high the fibres are not as easily distributed in the resin when mixing the charge, and mould filling becomes more difficult. Thus the glitch at 15% LPA could be due to several groups of fibre that did not distribute well, or to a random moulding error.

Figure 11 is a summary of the work done with LPA concentration and temperature profile[30] effects on LPA performance. *Figure 11* shows a plot of per cent final polymerization shrinkage (as measured by the

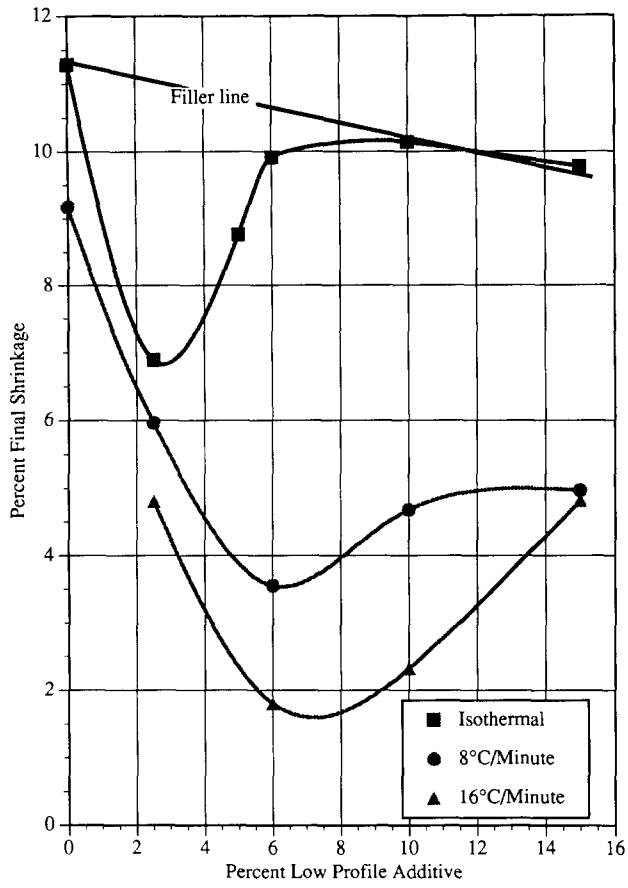

Figure 11 Summary of per cent final shrinkage data at various cure rates as a function of LPA concentration[30]

dilatometer) for the formulations in *Table 1* cured at isothermal, 8°C min^{-1} and 16°C min^{-1} ramping conditions. According to *Figure 11*, the LPA concentration should eventually reach an optimum for best shrinkage control, and with the addition of more LPA shrinkage control should lessen. As heating rate increased the minimum in shrinkage control broadened. Since the moulding was performed at 120°C, an approximate heating rate of 80°C min^{-1} would be an appropriate estimate. Extrapolating from *Figure 11*, one might guess that shrinkage at that rate should show a relatively wide minimum and a higher LPA concentration requirement. This is in agreement with the surface quality trends represented in *Figure 10*.

The D-sight index for the thickened panel was 471.9. This panel was moulded from charges containing 15% LPA and should be compared to the 15% LPA panel in *Figure 10*. Clearly, thickening markedly decreased the part-surface quality and the index value of the thickened part was nearly as poor as the 2.5% LPA panel. This is in agreement with the thickened dilatometry work described earlier.

Moulding shrinkage

Moulding shrinkage is a comparison between the cold-part dimensions to the cold-mould dimensions around the part perimeter. If the part dimensions are small compared to the mould, a shrinkage (negative number) is reported and if the part is dimensionally larger an expansion is reported (positive number). Moulding shrinkage is often used to describe the LPA effect on moulding, assuming that the better the LPA performance, the less moulding shrinkage one should measure.

Dimensions for moulding shrinkage are unit length over unit length. *Figure 10* provides a summary of the moulding shrinkage (multiplied by −1) measured. As was the case with surface quality, the best moulding shrinkage value was observed to be at an LPA concentration of 20%. Moulding shrinkage and D-sight index correlated nicely, as shown in *Figure 10*, implying that moulding shrinkage and surface quality were related. Comparing this plot to *Figure 11*, the trend seems to agree with the polymerization shrinkage measurement trends reported in ref. 30. Furthermore, the moulding shrinkage was much higher for the thickened panel (0.721E-3), again agreeing nicely with the surface quality data measured.

Surface area of moulded panels

The surface areas of the no LPA, 10% LPA, 20% LPA and 25% LPA panels were measured using the BET technique, as described earlier. Samples were prepared from material removed from the centre of the moulded panels and were broken and ground with a mortar and pestle. An effort was made to assure that the particle size distribution of the ground panel was about the same for each sample. The no LPA sample was included as a reference, as the inclusion of filler and fibre had an effect on the surface area of a sample without low-profile activity and the data discussed previously were for materials without filler and fibre. *Figure 12* is a plot comparing surface quality and surface area measured as

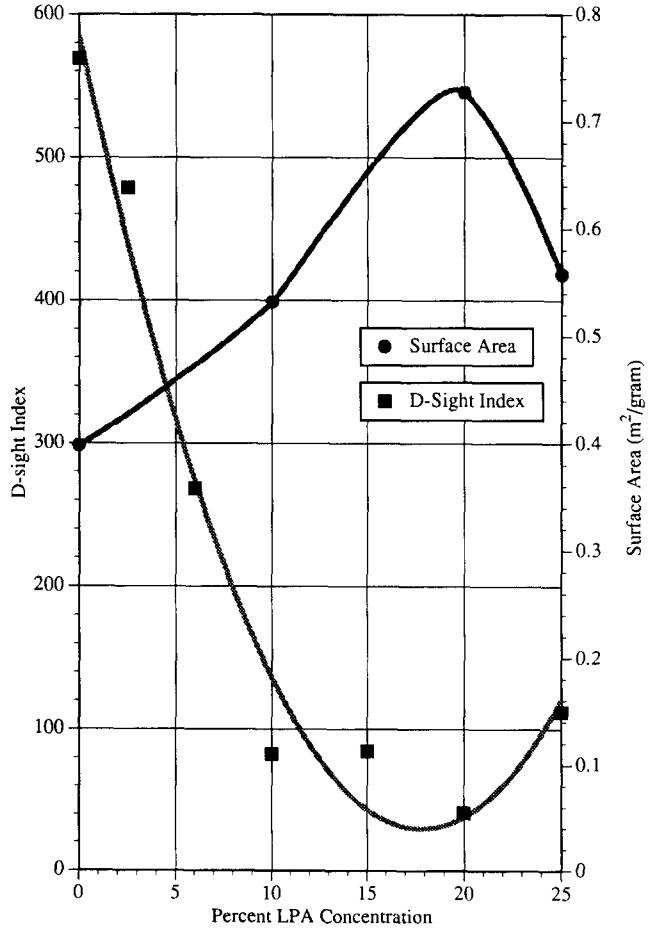

Figure 12 Comparison of D-sight index and surface area as a function of LPA concentration

a function of LPA content. The panel surface area correlated nicely with surface quality.

CONCLUSIONS

The effect of pressure and thickener on LPA performance was investigated as was the LPA mechanism. Pressure and thickening were found to have a negative effect on LPA performance. In investigating the LPA mechanism, it was found that the UP morphology did not change significantly once established during cure; however, sample appearance was found to change markedly, turning opaque during the plateau region. Based on the findings of this work and surface area measurements of some of the materials, an LPA mechanism was proposed which included first the microstructure formation followed by fissure formation in the LPA phase. The effects of morphology with respect to shrinkage control were explained in light of the mechanism. Finally, a series of BMC compression mouldings was performed to compare with the shrinkage trends measured with the dilatometer. Moulding shrinkage and moulded part-surface quality trends agreed with the polymerization shrinkage trends measured.

ACKNOWLEDGEMENTS

This research was supported by the Engineering Research Center for Net Shape Manufacturing at The Ohio State University and funds from Ashland Chemical Company and Union Carbide Corporation. The authors thank Ashland Chemical Company, Union Carbide Corporation and Atochem for material donations and Union Carbide Corporation for performing the BMC compression moulding.

REFERENCES

1 Kubel, E. *Adv. Mater. Process.* 1989, 17
2 *Burns, R. 'Polyester Molding Compound', Marcel Dekker, New York*, 1982
3 Atkins, K. in 'Sheet Molding Compound Materials: Science and Technology' (Ed. H. Kia), Hanser Publishers, Munich, 1993
4 Wood, S. *Modern Plastics* 1990, (Oct.), 50
5 Newman, S. and Fesko, D. *Polym. Comp.* 1984, **5** (1), 88
6 Landsettle, G. and Jensen, J. *Modern Plastics* 1986, (May), 80
7 Wood, S. *Modern Plastics* 1988, (Oct.), 46
8 Wigotsky, V. *Plast. Eng.* 1990, (Sept.), 19
9 Han, C. D. and Lem, K. *J. Appl. Polym. Sci.* 1983, **28**, 743
10 Lem, K. and Han, C. D. *J. Appl. Polym. Sci.* 1983, **28**, 779
11 Lee, D. and Han, C. D. *Polym. Eng. Sci.* 1987, **27** (13), 964
12 Melby, E. and Castro, J. in 'Comprehensive Polymer Science' (Ed. S. L. Aggarwal), Vol. 7, Pergamon Press, Oxford, 1989, Ch. 3
13 Hsu, C. P., Kinkelaar, M. and Lee, L. J. *Polym. Eng. Sci.* 1991, **31** (20), 1450
14 Kiaee, L., Yang, Y. S. and Lee, L. J. *AIChE Symp. Ser.* 1988, **84** (260), 52
15 Atkins, K., Gandy, R. and Gentry, R. European Patent Application no. 82108379, 1982
16 Suspene, L., Fourquier, D. and Yang, Y. S. *Polymer* 1991, **32**, 1593
17 Atkins, K., Koleske, J., Smith, P., Walter, E. and Mathews, V. 'Proceedings: SPI Composites Institute's 31st Annual Conference', 1976, Session 2-E
18 Atkins, K. United States Patent no. 4555534, 1985
19 Taylor, E. *Polym.-Plast. Technol. Eng.* 1984, **22** (1), 1
20 Rodriguez, E. *J. Appl. Polym. Sci.* 1990, **40**, 1847
21 Sawallisch, K. *Polym.-Plast Technol. Eng.* 1984, **23** (1), 1
22 Languna, O. and Collar, E. *J. Polym. Mater.* 1986, **3** (4), 217
23 Bush, S., Methven, J. and Blackburn, D. in 'Biological and Synthetic Polymer Networks' (Ed. S. O'Kremer), Elsevier Applied Science, New York, 1988
24 Grentzer, T., Gill, R., Sichina, W. and Sauerbrunn, S. 'Proceedings of the 4th Japan–US Conference on Composites', 1988, p. 458
25 Krolikowski, W. and Nowaczek, W. *Polym. Proc. Eng.* 1986, **4** (2–4), 295
26 Iseler, K., Guha, P. and Yen, R. United States Patent no. 4535110, 1985
27 Atkins, K. United States Patent no. 4491642, 1985
28 Bartkus, E. and Kroekel, C. *Appl. Polym. Symp.* 1970, **15**, 113
29 Mitani, T., Shiraishi, H., Honda, K. and Owens, G. 'Proceedings: SPI Composite Institute's 44th Annual Conference', 1989, Session 3-C
30 Kinkelaar, M. and Lee, L. J. *Polym. Eng. Sci.* in press
31 Fan, J. D. PhD Dissertation, The Ohio State University, 1988
32 Hsu, C. P. and Lee, L. J. *Polymer* 1993, **34**, 4516
33 Hsu, C. P. PhD Dissertation, The Ohio State University, 1992
34 Brunauer, S., Emmett, P. and Teller, E. *J. Am. Chem. Soc.* 1938, **60**, 309
35 Satterfield, C. 'Heterogeneous Catalysis – In Practice', McGraw Hill, New York, 1990
36 Accusorb System Manual, Micromeritics